Supporting Information

Self-curing solid-state electrolytes based on transamination bond exchange for reliable lithium batteries

Yu-Te Chen [a], Rohan Paste [a], Hong-Cheu Lin [a,b,*], Chih Wei Chu [c,d,e,f,*]

[a] *Department of Materials Science and Engineering, National Yang Ming Chiao Tung University, Hsinchu 300, Taiwan, ROC*

[b] *Center for Emergent Functional Matter Science, National Yang Ming Chiao Tung University, Hsinchu 300, Taiwan, ROC*

[c] *Research Center for Applied Sciences, Academia Sinica, No. 128, Sec. 2, Academia Road, Nangang, Taipei 11529, Taiwan, ROC*

[d] *College of Engineering, Chang Gung University, Taoyuan City 33302, Taiwan, ROC*

[e] *Center for Green Technology, Chang Gung University, Taoyuan City 33302, Taiwan, ROC*

[f] *Department of Photonics, National Yang Ming Chiao Tung University, Hsinchu 300, Taiwan, ROC*

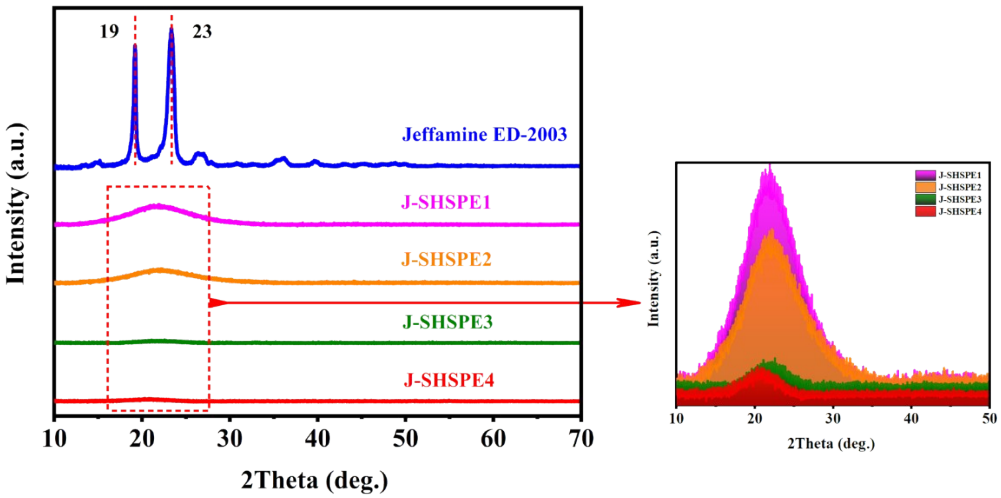

Figure S1. XRD pattern of the Jeffamine ED-2003, J-SHSPE1, J-SHSPE2, J-SHSPE3 and J-SHSPE4.

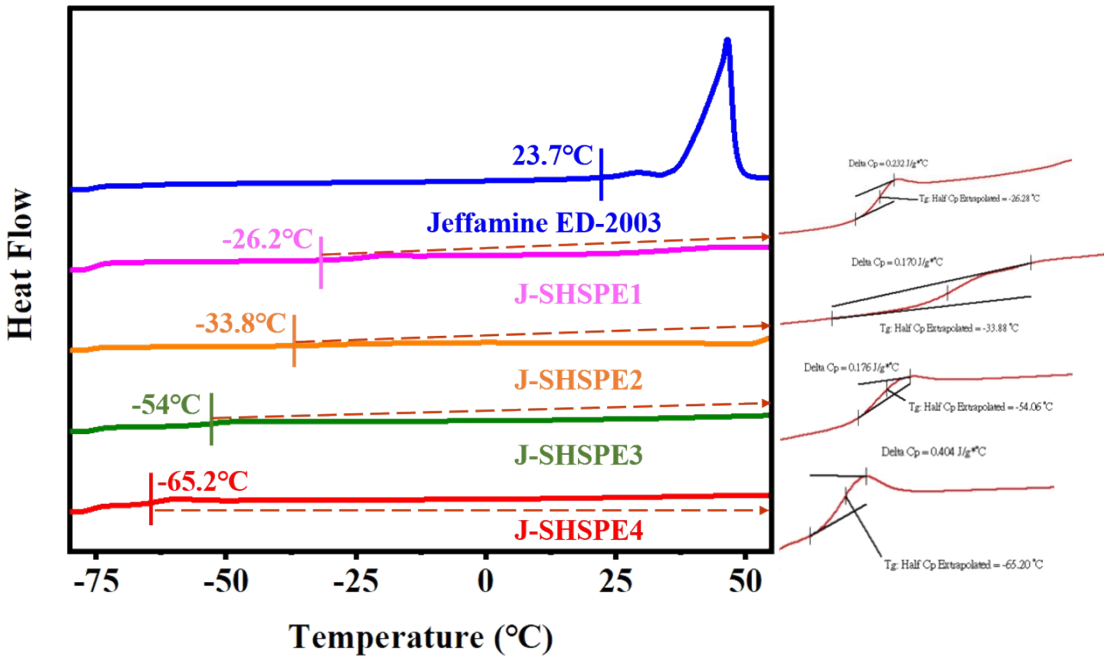

Figure S2. DSC curves of the Jeffamine ED-2003, J-SHSPE1, J-SHSPE2, J-SHSPE3 and J-SHSPE4.

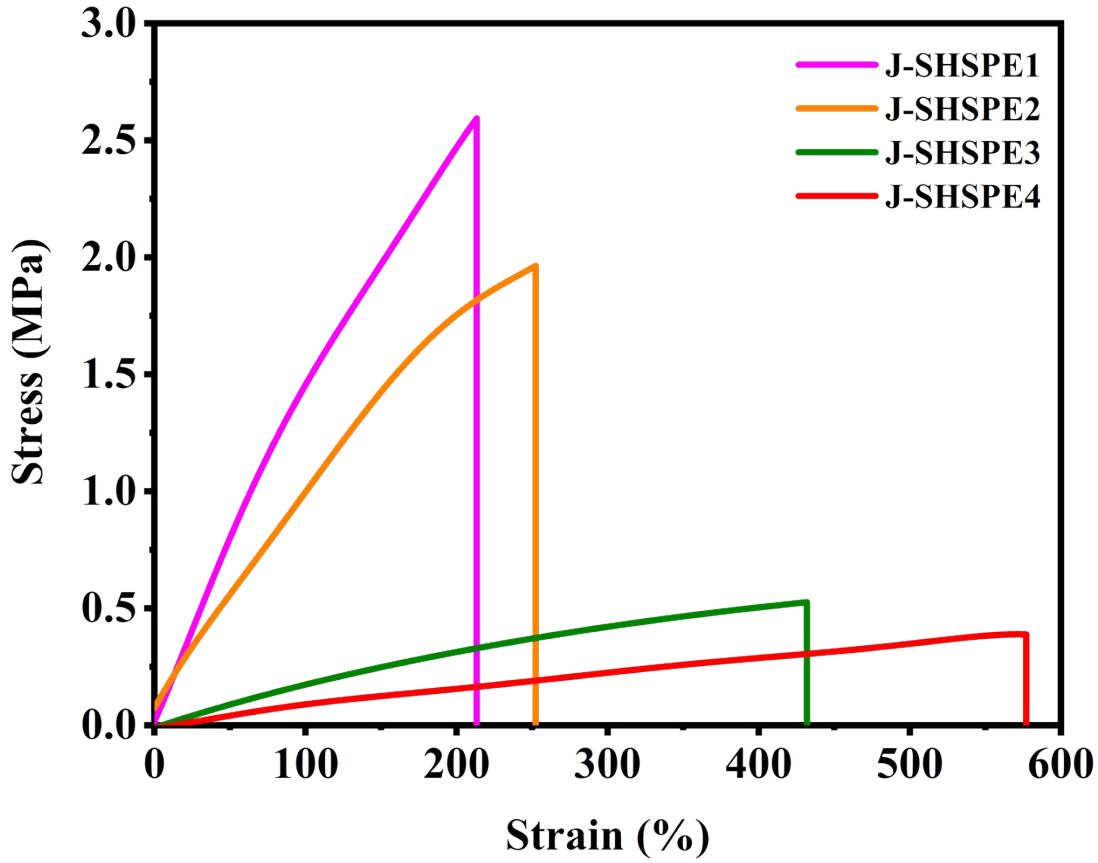

Figure S3. Stress/strain profiles of J-SHSPE1, J-SHSPE2, J-SHSPE3 and J-SHSPE4.

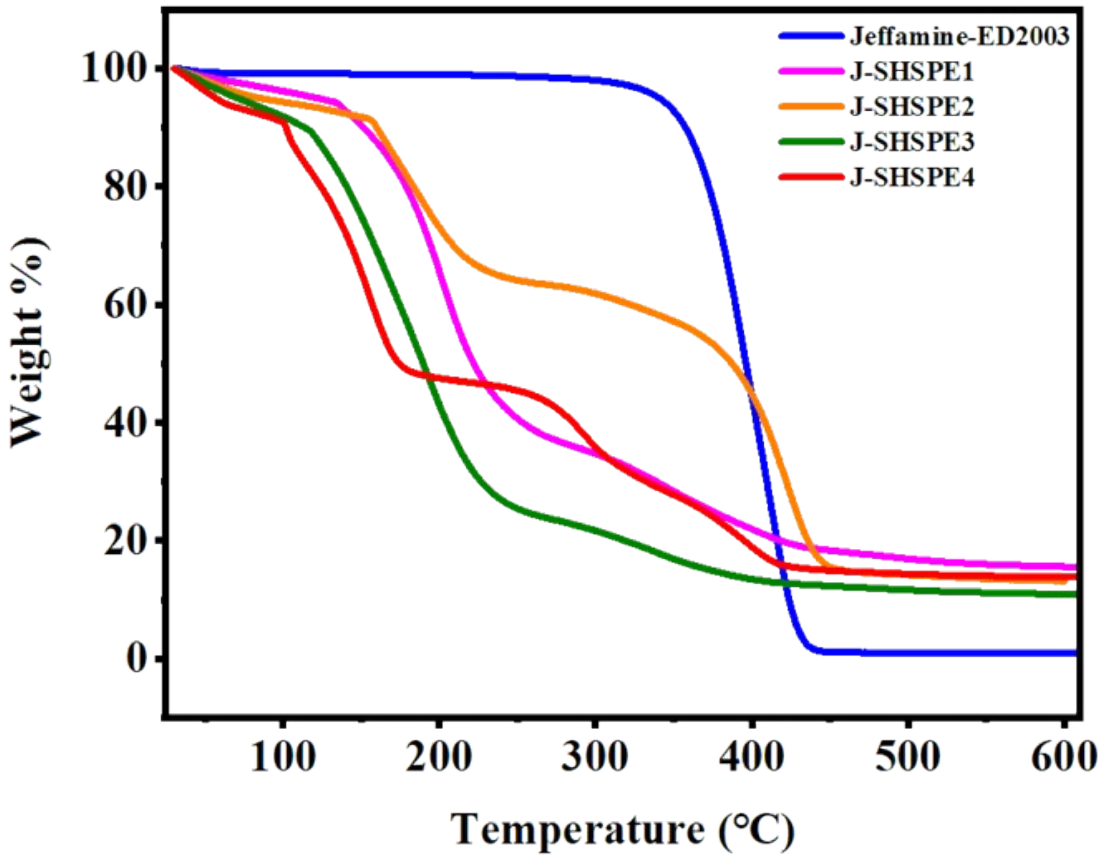

Figure S4. TGA profiles of the Jeffamine ED-2003, J-SHSPE1, J-SHSPE2, J-SHSPE3 and J-SHSPE4.

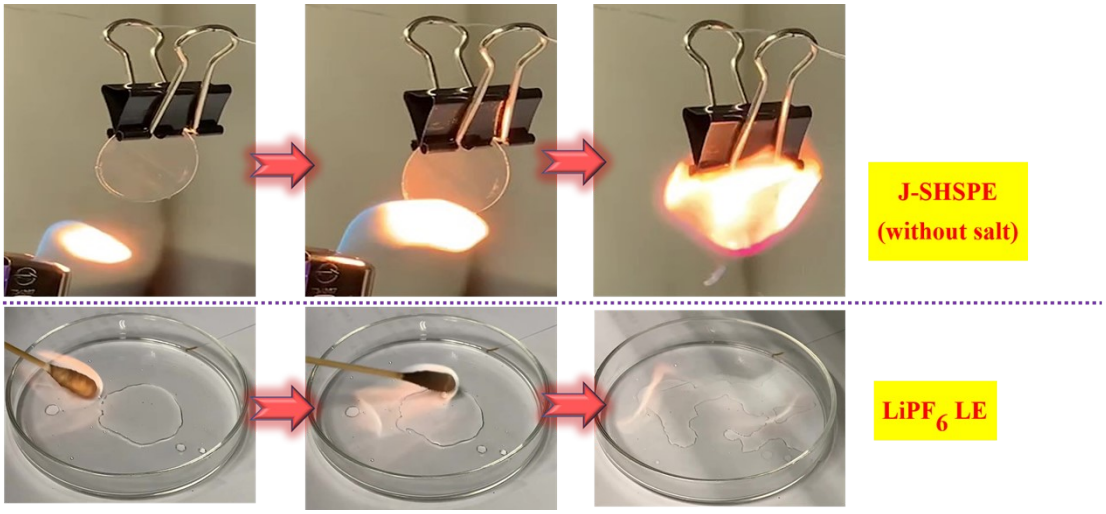

Figure S5. Combustion test of the J-SHSPE (without salt) and LE.

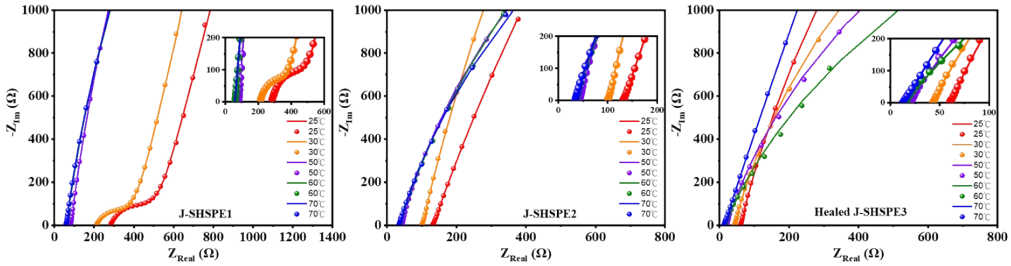

Figure S6. Selected temperature-dependent impedance spectra of the J-SHSPE1, J-SHSPE2 and healed J-SHSPE3 at 25–70 °C.

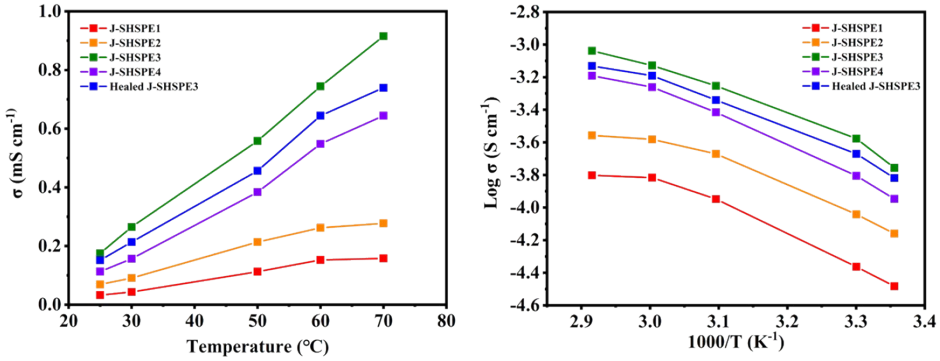

Figure S7. Ionic conductivity and corresponding Arrhenius plots at 25–70 ℃ of the J-SHSPE1, J-SHSPE2, J-SHSPE3, J-SHSPE4 and healed J-SHSPE3.

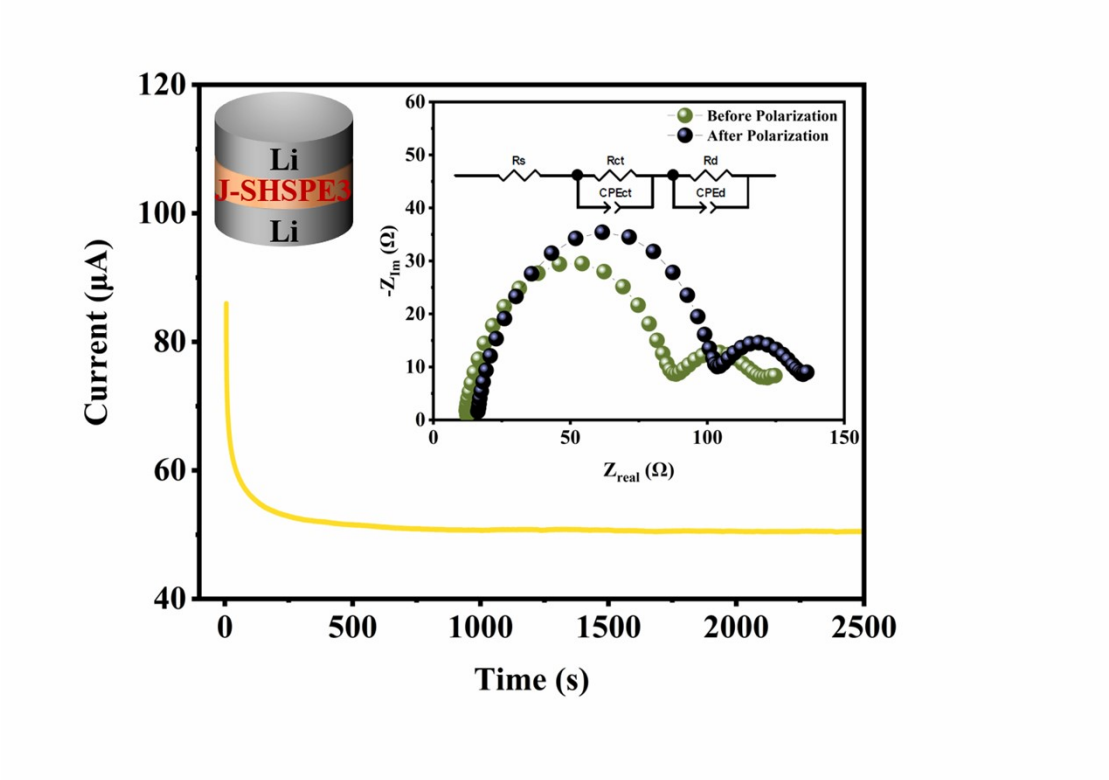

Figure S8. LITN of the Li/J-SHSPE3/Li at 30 ℃. Insert is impedance spectra before and after potential polarization.

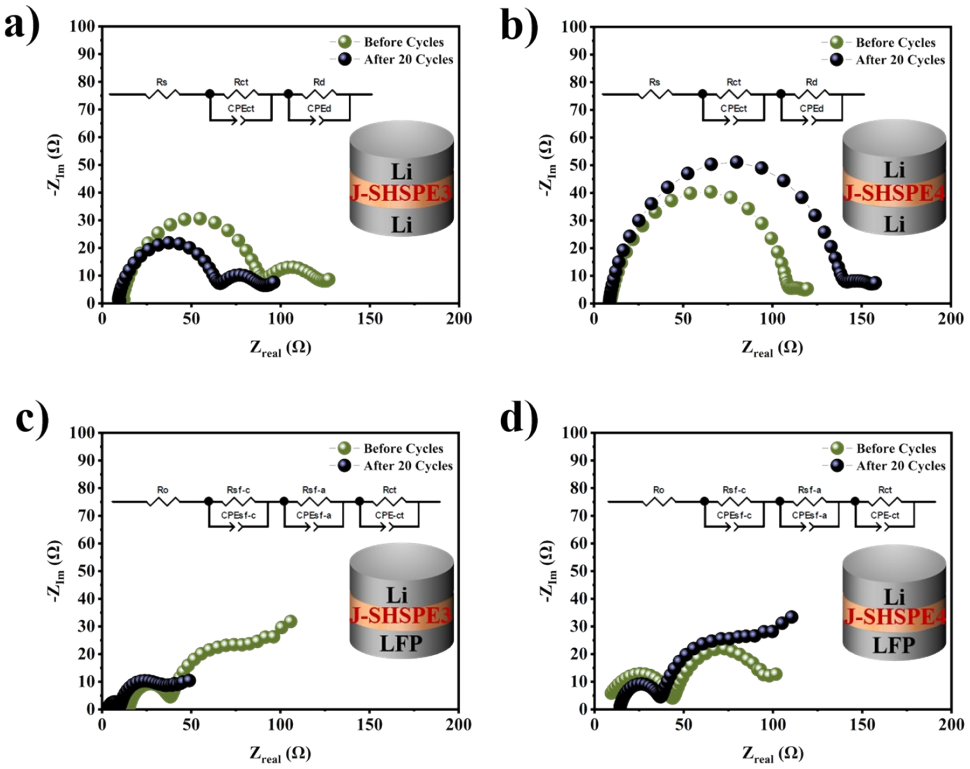

Figure S9. (a and b) EIS spectra of symmetric Li/J-SHSPE3/Li and Li/J-SHSPE4/Li cells before and after 20 cycles. (c and d) EIS spectra of asymmetric LFP/J-SHSPE3/Li cell and LFP/J-SHSPE4/Li cells before and after 20 cycles.

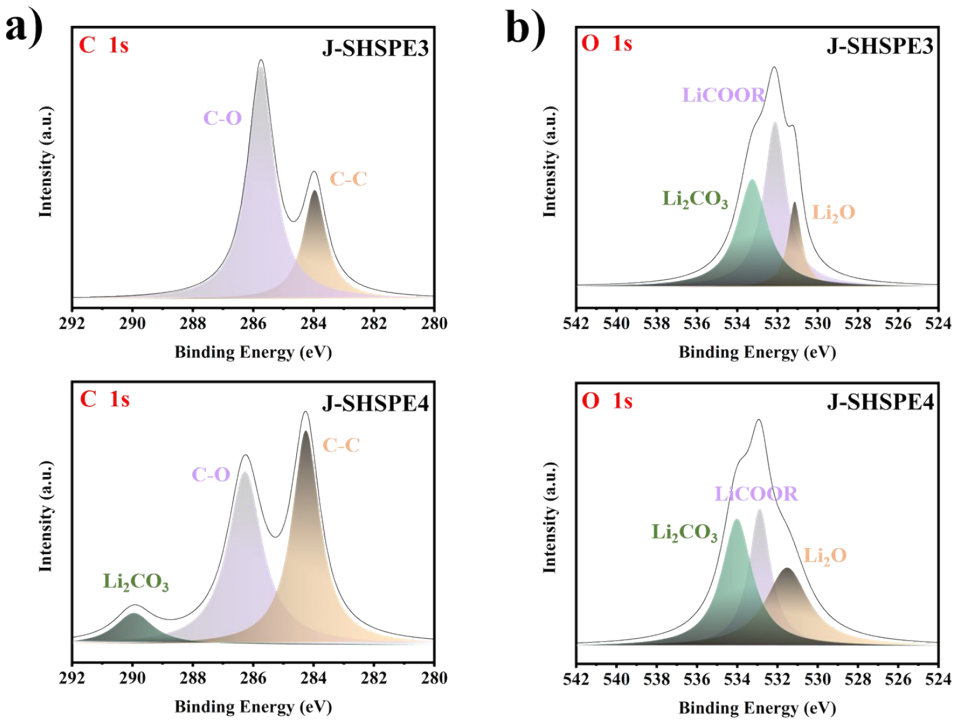

Figure S10. XPS analyses of J-SHSPE3 and J-SHSPE4 for a) the C 1s and b) the O 1s.

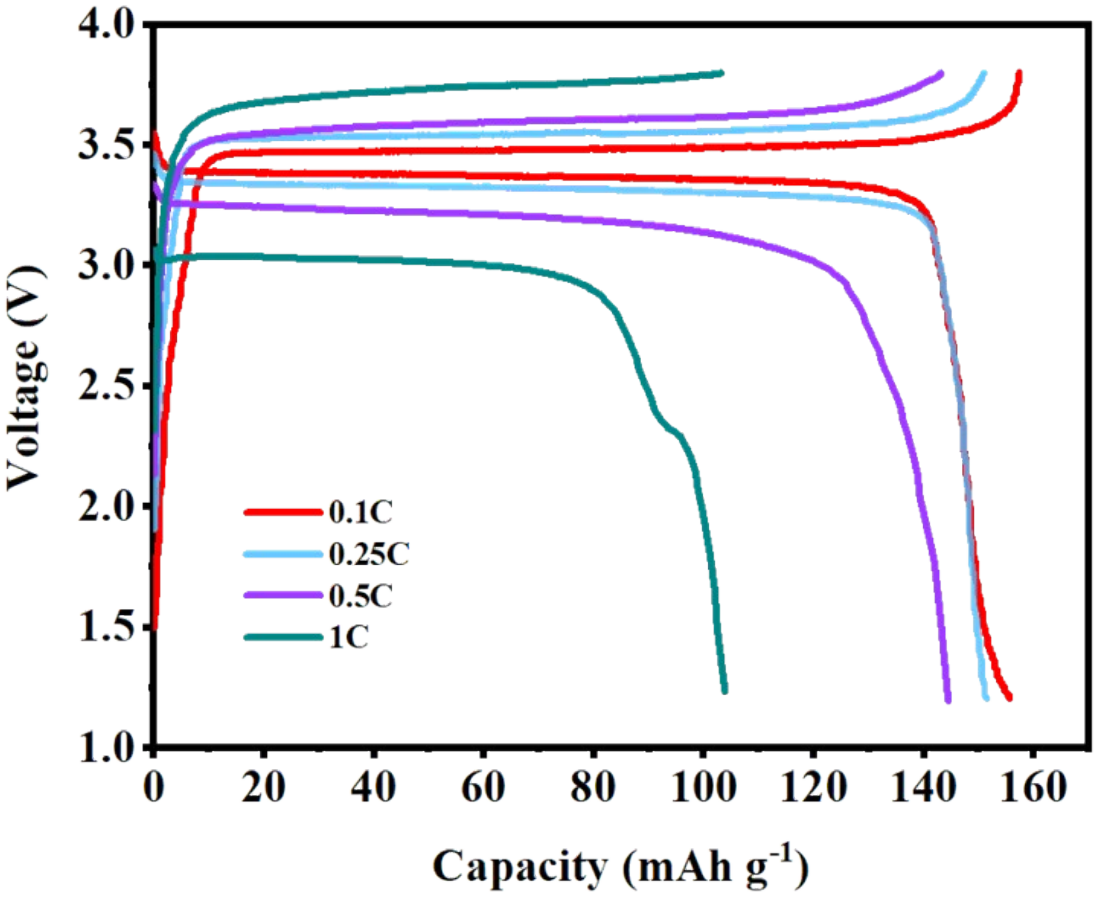

Figure S11. Galvanostatic charge/discharge curves of the J-SHSPE3.

Table S1. The detailed proportion of different J-SHSPEs.

Sample	The detailed proportion of different J-SHSPEs					
	Jeffamine® ED-2003	Benzene-1,3,5-tricarbaldehyde	$LiPF_6$ (LE)	DMF (solvent)	Volume ratio ($LiPF_6$ LE:DMF)	EO:Li
J-SHSPE1	950mg	50mg	3ml	7ml	3:7	7
J-SHSPE2	950mg	50mg	4ml	6ml	2:3	5
J-SHSPE3	950mg	50mg	5ml	5ml	1:1	4
J-SHSPE4	950mg	50mg	6ml	4ml	3:2	3

$LiPF_6$ (LE): 1M $LiPF_6$ in EC/EMC/DMC(1:1:1wt%)+1%VC

Table S2. The various values of the J-SHSPEs.

Sample	The various values of different J-SHSPEs				
	T_g (°C)	T_d (°C)	Toughness (J/m^3)	$Z_{real\ 30°C}$ (Ω)	$\sigma_{30°C}$ ($S\ cm^{-1}$)
J-SHSPE1	**-26.2**	**122.5**	**308**	**211.2**	**$4.3x10^{-5}$**
J-SHSPE2	**-33.8**	**86.1**	**293**	**100.7**	**$9.1x10^{-5}$**
J-SHSPE3	**-54**	**71.1**	**133**	**34.5**	**$2.7x10^{-4}$**
J-SHSPE4	**-65.2**	**57.1**	**121**	**58.4**	**$1.6x10^{-4}$**

Table S3. EIS-determined resistances of LFP/J-SHSPE3/Li and LFP/J-SHSPE4/Li, measured before and after 20 cycles.

Sample	$R_0(\Omega)$	$R_{sf\text{-}c}(\Omega)$	$R_{sf\text{-}a}(\Omega)$	$R_{ct}(\Omega)$
J-SHSPE3 (Before cycles)	14.99	38.82	101.3	23.4
J-SHSPE3 (After 20 cycles)	3.39	30.53	20.53	6.75
J-SHSPE4 (Before cycles)	6.52	13.67	23.06	58.4
J-SHSPE4 (After 20 cycles)	14.09	104.2	42.16	23.01

Electrolyte (polymer matrix)	σ (S cm^{-1})	Battery type (temperature)	Cycles (capacity retention)
J-SHSPE-3 (BTC-Jeffamine) (This work)	**2.7× 10^{-4}**	**LFP/Li (30 °C)**	**350 (85.6%)**
SIPE-5 (PEGMA-UPyMA-SSPSILi) [1]	1.2 × 10^{-6}	LFP/Li (60 °C)	60 (99.7 %)
SHSPE (PEG-BTA-NH_2) [2]	7.4 × 10^{-4}	LFP/Li (27 °C)	300 (84.3 %)
shPE (UPyMA-PEGMA) [3]	2.1 × 10^{-4}	LFP/Li (60 °C)	100 (91.1%)
SHSPE (PEG-TPU-IPDI) [4]	1.9 × 10^{-4}	LFP/Li (60 °C)	100 (90 %)
SHCPE-10 (PEG-UPy/SiO_2-UPy) [5]	8 × 10^{-5}	LFP/Li (60 °C)	60 (87.3%)
DN-SHPE (PEGBCDMA-PEGDA) [6]	2.9 × 10^{-5}	LFP/Li (60 °C)	120 (92.8%)
PVT-EMIMTFSI (PVT/EMIMTFSI) [7]	1.2 × 10^{-4}	LFP/Li (25 °C)	40 (-)
CPSHPE (HCP-UPyMA-PEGMA) [8]	8.9 × 10^{-5}	LFP/Li (60 °C)	70 (87.7%)
SHSPEs (PEGSS-PEGDMA) [9]	7.2 × 10^{-6}	LFP/Li (60 °C)	100 (97.5%)
ShSPE (TPA-PEG-DGEBA) [10]	1.6 × 10^{-4}	LFP/Li (60 °C)	50 (85.2%)
SSSPE (PVA-UPy-PEG) [11]	1.5 × 10^{-4}	LFP/Li (60 °C)	150 (80.6%)
SHSPE (poly(HFBM-co-SBMA)) [12]	8 × 10^{-6}	LFP/Li (60 °C)	100 (82%)

Table S4. Summary of SHSPE-based LFP batteries.

REFERENCES

[1] H. Gan, Y. Zhang, S. Li, L. Yu, J. Wang, Z. Xue, ACS Appl. Energy Mater., 4 (2021) 482-491.

[2] L. Zhang, P. Zhang, C. Chang, W. Guo, Z.H. Guo, X. Pu, ACS Appl. Mater. Interfaces, 13 (2021) 46794-46802.

[3] B. Zhou, D. He, J. Hu, Y. Ye, H. Peng, X. Zhou, X. Xie, Z. Xue, J. Mater. Chem. A, 6 (2018) 11725-11733.

[4] N. Wu, Y.-R. Shi, S.-Y. Lang, J.-M. Zhou, J.-Y. Liang, W. Wang, S.-J. Tan, Y.-X. Yin, R. Wen, Y.-G. Guo, Angew. Chem. Int. Ed., 58 (2019) 18146-18149.

[5] B. Zhou, Y.H. Jo, R. Wang, D. He, X. Zhou, X. Xie, Z. Xue, J. Mater. Chem. A, 7 (2019) 10354-10362.

[6] B. Zhou, C. Zuo, Z. Xiao, X. Zhou, D. He, X. Xie, Z. Xue, Chem. Eur. J., 24 (2018) 19200-19207.

[7] X. Tian, P. Yang, Y. Yi, P. Liu, T. Wang, C. Shu, L. Qu, W. Tang, Y. Zhang, M. Li, B. Yang, J. Power Sources, 450 (2020) 227629.

[8] B. Zhou, M. Yang, C. Zuo, G. Chen, D. He, X. Zhou, C. Liu, X. Xie, Z. Xue, ACS Macro

Lett., 9 (2020) 525-532.

[9] Y.H. Jo, S. Li, C. Zuo, Y. Zhang, H. Gan, S. Li, L. Yu, D. He, X. Xie, Z. Xue, Macromolecules, 53 (2020) 1024-1032.

[10] X. Cao, P. Zhang, N. Guo, Y. Tong, Q. Xu, D. Zhou, Z. Feng, RSC Adv., 11 (2021) 2985-2994.

[11] Y.H. Jo, B. Zhou, K. Jiang, S. Li, C. Zuo, H. Gan, D. He, X. Zhou, Z. Xue, Polym. Chem., 10 (2019) 6561-6569.

[12] C. Wang, R. Li, P. Chen, Y. Fu, X. Ma, T. Shen, B. Zhou, K. Chen, J. Fu, X. Bao, W. Yan, Y. Yang, J. Mater. Chem. A, 9 (2021) 4758-4769.